



Updated emission inventories of power plants in simulating air quality during haze periods over East China

Lei Zhang^{1,2}, Tianliang Zhao^{1,2}, Sunling Gong³, Shaofei Kong^{1,2,4}, Lili Tang⁵, Duanyang Liu⁶, Yongwei Wang², Lianji Jin², Yunpeng Shan⁷, Chenghao Tan^{1,2}, Yingjie Zhang^{1,2}, and Xiaomei Guo⁸

¹Climate and Weather Disasters Collaborative Innovation Center, Nanjing University of Information Science & Technology, Nanjing, 210044, China

²Key Laboratory for Aerosol-Cloud-Precipitation of China Meteorological Administration, Nanjing, 210044, China

³Key Laboratory for Atmospheric Chemistry, Chinese Academy of Meteorological Sciences, Beijing, 100081, China

⁴Department of Atmospheric Sciences, School of Environmental Studies, China University of Geosciences, Wuhan, 430074, China

⁵Jiangsu Environmental Monitoring Center, Nanjing, 210036, China

⁶Observatory of Jiangsu Province, Nanjing, 210008, China

⁷Division of Atmospheric Science, Desert Research Institute, Reno, Nevada 89512, USA

⁸Weather Modification Office of Sichuan Province, Chengdu, 610072, China

Correspondence: Tianliang Zhao (tlzhao@nuist.edu.cn) and Shaofei Kong (kongshaofei@cug.edu.cn)

Received: 8 February 2017 – Discussion started: 24 April 2017

Revised: 24 December 2017 – Accepted: 5 January 2018 – Published: 13 February 2018

Abstract. Air pollutant emissions play a determinant role in deteriorating air quality. However, an uncertainty in emission inventories is still the key problem for modeling air pollution. In this study, an updated emission inventory of coal-fired power plants (UEIPP) based on online monitoring data in Jiangsu Province of East China for the year of 2012 was implemented in the widely used Multi-resolution Emission Inventory for China (MEIC). By employing the Weather Research and Forecasting model with Chemistry (WRF-Chem), two simulation experiments were executed to assess the atmospheric environment change by using the original MEIC emission inventory and the MEIC inventory with the UEIPP. A synthetic analysis shows that power plant emissions of PM_{2.5}, PM₁₀, SO₂, and NO_x were lower, and CO, black carbon (BC), organic carbon (OC) and NMVOCs (non-methane volatile organic compounds) were higher in UEIPP relative to those in MEIC, reflecting a large discrepancy in the power plant emissions over East China. In accordance with the changes in UEIPP, the modeled concentrations were reduced for SO₂ and NO₂, and increased for most areas of primary OC, BC, and CO. Interestingly, when the UEIPP was used, the atmospheric oxidizing capacity significantly reinforced. This was reflected by increased oxidizing agents, e.g., O₃

and OH, thus directly strengthening the chemical production from SO₂ and NO_x to sulfate and nitrate, respectively, which offset the reduction of primary PM_{2.5} emissions especially on haze days. This study indicates the importance of updating air pollutant emission inventories in simulating the complex atmospheric environment changes with implications on air quality and environmental changes.

1 Introduction

East China is one of the regions with serious air pollution and frequent haze. In these highly polluted regions, air pollutant emissions play a key role in air quality, and their variations can cause a large uncertainty in air pollution modeling and prediction. It is also crucial for air pollution mitigation to comprehensively understand air pollutant emissions and their impacts on the atmospheric environment. Emission inventories are essential for atmospheric environment research, especially for modeling studies and air quality policy decisions.

During past decades, emission inventories for China were established by several groups. These include the global-scale

studies, such as the Reanalysis of the Tropospheric chemical composition (RETRo; Schultz, 2007; Zheng et al., 2009), the Hemispheric Transport of Air Pollution (HTAP; Janssens-Maenhout et al., 2015) and the Emission Database for Global Atmospheric Research (EDGAR), and the national-scale studies including the Transport and Chemical Evolution over the Pacific mission (TRACE-P; Olivier et al., 2005), the Intercontinental Chemical Transport Experiment-Phase B (INTEX-B; Zhang et al., 2009), the Regional Emission inventory in Asia (REAS; Ohara et al., 2007) and the Multi-resolution Emission Inventory for China (MEIC, <http://www.meicmodel.org/>). Owing to poor measurements, several of these studies were based on a “top-down” algorithm, which rendered the uncertainties in estimation of emissions and subsequently decreased the accuracy in modeling the atmospheric environment. For example, previous studies showed a difference of 30 % in CO emission among various emission inventories over east Asia, leading to an up to 8 % simulated deviation (Amnuaylojaroen et al., 2014). Regional emission inventories were developed recently in China, for the regions of the Yangtze River Delta (Huang et al., 2011; Fu et al., 2013), the North China Plain (Wang et al., 2010) and the Pearl River Delta (Zheng et al., 2009), as well as several provincial and urban areas (Zhao et al., 2015; Jing et al., 2016; He et al., 2016), with more underlying data obtained for activity levels, emission factors, energy combustion, and traffic.

Air pollution in East China is changing from coal-smoke to mix-source pollution, particularly the secondary aerosols surging in severe haze episodes (R.-J. Huang, et al., 2014), with more complicated chemical reactions involved in the interaction of particle formation and O₃ production. As the largest coal-fired sector of the emission framework in China, electric power generation is believed to be the most important source of atmospheric pollutant emissions (Zhao et al., 2010). Power plant emissions accounted for 31–59 % of national anthropogenic emissions of SO₂ and 21–44 % of NO_x (Zhao et al., 2008; Wang et al., 2012). The pollutant emissions from coal-fired power plants were usually estimated by the widely adopted “bottom-up” approach (Hao et al., 2002; Zhang et al., 2007a, b; Ohara et al., 2007; Zhao et al., 2008). However, due to limited access to specific information about power plants, such as the mass of pollutant emitted per unit fuel consumption or per unit industrial production, coal-fired boiler types or accurate locations of power plants (Wang et al., 2012), the uncertainty and inaccuracy of emissions from local power plants can lead to model bias. The validations of power plant emissions with the impacts on atmospheric environment particularly in haze episodes are still unknown.

Jiangsu Province is one of the most developed areas in East China, providing a living place for a population of 79.2 million people with the highest gross domestic production per capita in China (NBS, 2013; JSNBS, 2013). Severe air pollution episodes of haze and photochemical pollution have shrouded this province in recent years (Fu et al., 2008; Wang

et al., 2014; Qi et al., 2015). As elevated emission sources, power plants emit air pollutants with longer life cycles in the upper air and more efficiently transport across regions because of less deposition driven by stronger winds and a well organized circulation in the upper air, e.g., by low-level jets (Hu et al., 2013). This leads to more significant environmental effects than surface emissions (e.g., on-road emissions), reflecting the potential importance of accurately estimating the power plant emissions and their influences on air quality. Based on a unit-based methodology, Zhao et al. (2008) developed an inventory of coal-consuming power plants for all the provinces in China. The annual SO₂ and NO_x emissions were estimated as 1107 and 626 kt (kilotons), respectively, in 2005, as well as 803 and 781 kt, respectively, in 2010 in Jiangsu Province. Alternately, another study estimated NO_x emissions in the province at about 748 kt in 2005 (Wang et al., 2012), reflecting the uncertainties in estimation of NO_x emissions from power plants. Source control measures focusing on power generation processes and facility-related measures to reduce emissions have been widely implemented in China. These measures include flue-gas desulfurization (FGD), selective catalytic reduction (SCR), selective non-catalytic reduction (SNCR), dust collectors, etc. It is important to assess the potential air-quality changes from implementation of these mitigation measures.

Y. Zhang et al. (2015) established an emission inventory of coal-fired power plants (UEIPP) by collecting the online monitoring data from power plants in atmospheric verifiable accounting tables of Jiangsu Province for 2012. The volumes of flue-gas and pollutant concentrations were measured on-site for each unit, providing the more realistic data for calculating power plant emissions than those used in previous studies. As a major objective of this study, the UEIPP was integrated into MEIC to evaluate the impact of updated emissions on the regional atmospheric environment with an air-quality model. We present the details of model settings, observational data and emission inventories in Sect. 2 and the modeling evaluation in Sect. 3. The impact of emissions change on the atmospheric environment and the underlying mechanism are discussed in Sect. 4. The study is summarized in Sect. 5.

2 Data and methods

2.1 Model description and configuration

The period from 29 November to 31 December 2013 was chosen as the modeling period, covering a severe haze period (from 3 to 8 December 2013) in Jiangsu Province. The online coupled Weather Research and Forecasting Model with Chemistry (WRF-Chem in version 3.7.1) was configured in three nesting domains with horizontal resolutions of 45 km covering most areas of east Asia, 15 km covering eastern China and surrounding areas, and 5 km covering Jiangsu

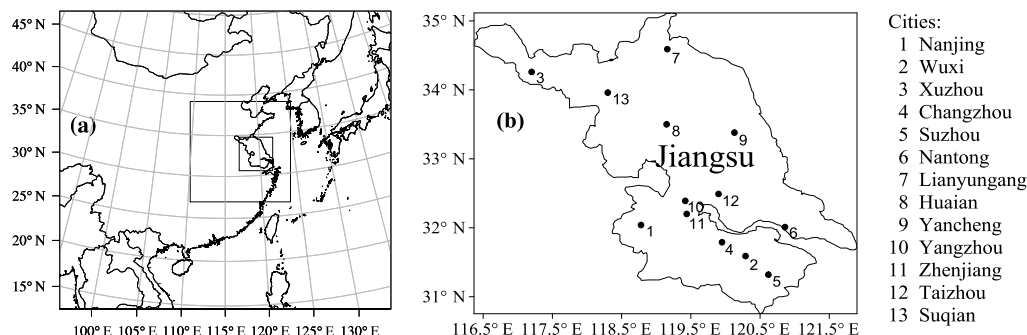


Figure 1. Model domain and the locations of the 13 cities in Jiangsu Province.

Province and surrounding areas (Fig. 1a). Vertically, there were 35 full eta levels from surface up to 100 hPa with 7 levels below 1 km. The National Center for Environmental Prediction Final Global Forecast System operational analysis data (Kalnay et al., 1996) was utilized for providing the initial and lateral meteorological conditions to WRF-Chem. Grid nudging (Stauffer and Seaman, 1990) was employed for the outermost domain every 6 h (treating temperature, horizontal wind, and water vapor) to guarantee the precision of large-scale meteorology during the simulations.

The selected physical configurations included the Morrison double-moment microphysics scheme (Morrison et al., 2009), RRTMG (Rapid Radiative Transfer Model for GCMs – global climate models), long- and short-wave radiation scheme (Iacono et al., 2008), Grell 3-D cumulus parameterization, the Yonsei University planetary boundary layer scheme (Hong et al., 2006), and the Noah land surface model. For the chemistry and aerosol mechanisms, the CBM-Z (Carbon Bond Mechanism version Z; Zaveri, 1999) coupling with the 8-bin sectional MOSAIC (Model for Simulating Aerosol Interactions and Chemistry) with aqueous chemistry (Zaveri et al., 2008) was used. The MOSAIC, treating all the important aerosol components including nitrate, sulfate, ammonium, black carbon (BC), and primary organic aerosols and other inorganic aerosols, is efficient without compromising accuracy and widely used in air-quality and regional or global aerosol models (Zaveri et al., 2008). Since the MOSAIC is incapable of simulating secondary organic aerosols (SOAs), the simulated organic aerosols mentioned hereinafter all refers to primary organic aerosols. The crucial processes of radiation feedback, aerosol and cloud interaction, dry deposition, wet scavenging and cloud chemistry were turned on. Biogenic emissions were calculated online with MEGAN (Model of Emission of Gases and Aerosol from Nature; Guenther et al., 2006). The initial and boundary chemistry conditions were based on the vertical profiles of O₃, SO₂, NO₂, VOCs (volatile organic compounds) and other air pollutants from the NOAA Aeronomy Lab Regional Oxidant Model (NALROM; Liu et al., 1996). The first 2-day simulation was discarded as the spin-up. The outermost do-

main of modeling tests was set large enough to cover east Asia to avoid the influence of chemical boundary conditions on the simulation. Furthermore, the frequent haze pollution over eastern China is a result from the regional pollutant emissions (Wang et al., 2015; Q. Zhang et al., 2015) with less contribution of foreign emissions to haze pollution over eastern China.

2.2 Observational data

Meteorological fields simulated by the model are crucial for the accuracy of air-quality modeling. In the southern, middle, and northern parts of Jiangsu Province, we selected the three prefecture-level cities of Nanjing, Yancheng, and Lianyungang, respectively, to evaluate the overall perspective of meteorological simulation with the available observations. The observed meteorological data, involving 2 m temperature, 2 m relative humidity and 10 m wind speed and direction were collected from the Jiangsu Provincial Meteorological Bureau and Meteorological Information Comprehensive Analysis and Process System (MICAPS) of the China Meteorological Administration (CMA). Hourly surface concentrations of chemical species in 13 cities of Jiangsu, including SO₂, NO₂, PM_{2.5}, CO and O₃, were obtained from the Jiangsu Environmental Protection Bureau. Daily secondary inorganic aerosols (SIAs; sulfate, nitrate, ammonium) in PM_{2.5} were measured using MARGA (Online Analyzer of Monitoring of Aerosol and Gases) at Jiangsu Environmental Monitoring Center. MARGA is a fully autonomous sampling and measurement system that continuously measures the gases (HCl, HNO₃, HNO₂, SO₂, and NH₃) and aerosol components (Cl⁻, NO³⁻, SO₄²⁻, NH⁴⁺, K⁺, Ca²⁺, and Mg²⁺) by ion chromatography and the internal standard eliminates the need for calibration.

2.3 Air pollutant emission inventory

2.3.1 Two inventories for power plant emissions

This study uses the MEIC inventory as the default anthropogenic emissions including the emissions of sulfur diox-

ide (SO_2), nitrogen oxides (NO_x), carbon monoxide (CO), ammonia (NH_3), black carbon (BC), organic carbon (OC), non-methane volatile organic compounds (NMVOCs), $\text{PM}_{2.5}$, and PM_{10} by five sectors of power, industry, transportation, residential, and agriculture.

The UEIPP in Jiangsu Province for the year of 2012 consisting of six online species (SO_2 , NO_x , $\text{PM}_{2.5}$, PM_{10} , BC, and OC) was established using the online monitoring data of three pollutants (SO_2 , NO_x , and total suspended particles – TSP) and the volume of flue gases on power plant and daily levels (Y. Zhang et al., 2015). Atmospheric verifiable accounting tables, comprising accurate locations, boiler type, coal consumption, and control policies for individual plants were adopted to calculate the CO and NMVOCs emissions in UEIPP (Y. Zhang et al., 2015).

The SO_2 , NO_x , and TSP emissions were estimated directly from online concentrations and volumes of flue gases as follows:

$$E_{i,j,k} = A_{i,j,k} \cdot c_{i,j,k}, \quad (1)$$

where $A_{i,j,k}$ is the daily emitted volume of flue gas and $c_{i,j,k}$ is the daily concentration, with i , j , and k representing the pollutant species, individual plant, and day, respectively. The emissions of $\text{PM}_{2.5}$, PM_{10} , BC, and OC were then calculated using the online TSP emissions

$$E_{i,j,k} = T_{i,j,k} \cdot P_i, \quad (2)$$

where $T_{i,j,k}$ stands for the online TSP emissions and P_i represents the $\text{PM}_{2.5}$, PM_{10} , BC, and OC mass ratios to TSP. The online monitoring system is currently incapable of providing the mass ratios on the power plant and thus it is given as a unified value referring to the work of Y. Zhang et al. (2015) for each of the four species, which was 52.7 % ($\text{PM}_{2.5}$), 80.4 % (PM_{10}), 8.6 % (BC), and 6.1 % (OC).

The annual emissions of CO and NMVOCs were calculated using Eq. (3):

$$E_{i,j,k} = A_{i,j,k} \cdot \text{EF}_{i,j,k} \cdot (1 - \eta_{i,j,k}), \quad (3)$$

where $A_{i,j,k}$ is the activity level, $\text{EF}_{i,j,k}$ is the uncontrolled emission factor and $\eta_{i,j,k}$ is the removal efficiency of the air pollutant control device. In reference to previous studies (Wang et al., 2005; Streets et al., 2006; Bo et al., 2008; Huang et al., 2011), the $\text{EF}_{i,j,k}$ of CO and NMVOCs were set at 4.03 and 0.12 g kg^{-1} , respectively, and $\eta_{i,j,k}$ was set to 0.

Following the method used by Li et al. (2014) and the mechanism-dependent mapping tables developed by Carter (2013), the NMVOCs in UEIPP were specified to individual constituents in the Regional Acid Deposition Model chemical mechanism (RADM2; Stockwell et al., 1990), which could be adapted to the WRF-Chem/CBM-Z mechanism used in this study. The primary distinction between UEIPP and the power plant emission inventory estimated in

Table 1. The UEIPP and MEIC power plant emissions of major air pollutants as well as the ratios in total emission inventory over Jiangsu Province in 2012.

| | UEIPP | | MEIC power plant emissions | |
|-------------------|-------------------------------------|-----------------------|-------------------------------------|-----------------------|
| | Emission (kt yr^{-1}) | Ratio in total (%) | Emission (kt yr^{-1}) | Ratio in total (%) |
| SO_2 | 105.6 | 10.4 | 367.8 | 28.8 |
| $\text{PM}_{2.5}$ | 21.6 | 3.7 | 72.2 | 11.3 |
| PM_{10} | 32.6 | 4.0 | 103.7 | 11.6 |
| NO_x | 277.9 | 17.2 | 733.8 | 35.4 |
| CO | 582.0 | 6.2 | 343.5 | 3.7 |
| BC | 3.6 | 4.3 | 0.1 | 0.2 |
| OC | 2.5 | 1.7 | 0.0 | 0.0 |
| NMVOCs | 17.3 | 0.9 | 7.2 | 0.4 |

previous China studies lies in the different data used and subsequently the estimation algorithm as well as the temporal resolution. Previously, the power plant emission inventory was mostly estimated using various data such as activity levels, boiler types, fuel types, control policies, and emission factors, and the activity levels were usually collected on annual or monthly timescales. In the UEIPP, the emissions of SO_2 , NO_x , $\text{PM}_{2.5}$, PM_{10} , BC, and OC were calculated using the online pollutant concentrations and volume of flue gases on a daily timescale. Rejection heights of the UEIPP and the original power plant emission in MEIC were set at about 100 and 200 m, respectively, above ground, corresponding to the second and third model levels for this WRF-Chem simulation.

2.3.2 Differences between the two power plant emission inventories

The UEIPP and MEIC power plant emissions of major air pollutants with their fractions in the total emissions over Jiangsu Province in 2012 are presented in Table 1. Appreciable differences between the two power plant emission inventories were revealed. The power plant emissions of SO_2 , $\text{PM}_{2.5}$, PM_{10} , and NO_x in the MEIC are 367.8, 72.2, 103.7, and 733.8 kt, respectively, and reducing to 105.6, 21.6, 32.6, and 277.9 kt, respectively, in the UEIPP. The notable reductions of SO_2 and NO_x may largely be due to comprehensive implementation of FGD and SCR/SNCR in Jiangsu Province, which was not captured in the national inventory. Application rate and average SO_2 removal efficiency of FGD in coal-fired power plants were obviously higher than those in other sectors (Zhou et al., 2017), further confirmed by the abrupt decrease in SO_2 power plant emissions in China since 2006 (Liu et al., 2015). Differences also existed in the estimation of NO_x removal efficiency of SCR/SNCR for power plants in Jiangsu in 2012 among different studies, reflecting 37 % (average of SCR/SNCR) calculated by Zhou et al. (2017), while 70 % (SCR) and 25 % (SNCR) calculated by Tian et al. (2013). In addition, due to inconsistent pen-

Table 2. Statistics between observed (Obs.) and modeled (Mod.) meteorology.

| | Nanjing | | | | | Yancheng | | | | | Lianyungang | | | | |
|-------------------------|---------|------|------|------|------|----------|------|------|------|------|-------------|------|------|------|------|
| | Obs. | Mod. | MB | R | RMSE | Obs. | Mod. | MB | R | RMSE | Obs. | Mod. | MB | R | RMSE |
| T (°C) | 4.8 | 3.8 | -1.0 | 0.86 | 3.0 | 4.4 | 5.5 | 1.1 | 0.94 | 2.0 | 3.4 | 2.9 | -0.5 | 0.90 | 2.3 |
| RH (%) | 63.0 | 63.6 | 0.6 | 0.79 | 14.6 | 64.3 | 58.6 | -5.7 | 0.79 | 14.4 | 56.4 | 58.2 | 1.8 | 0.82 | 18.2 |
| WS (m s ⁻¹) | 2.0 | 3.1 | 1.1 | 0.51 | 1.8 | 3.0 | 4.3 | 1.3 | 0.77 | 2.0 | 2.0 | 3.8 | 1.4 | 0.56 | 2.1 |

* T: temperature at 2 m; RH: relative humidity at 2 m; WS: wind speed at 10 m; MB: mean bias; R: correlation coefficient; RMSE: root mean square error; all R values passed $p < 0.001$.

tration rates and removal efficiencies of dust collectors determined on national and provincial levels, there also remained discrepancies in the estimation of PM_{2.5} and PM₁₀ emissions (Xia et al., 2016; Zhou et al., 2017). However, the bias could be avoided in the UEIPP (see Sect. 2.3.1 for details). The UEIPP produced higher CO (582.0 kt), BC (3.6 kt), OC (2.5 kt), and NMVOCs (17.3 kt) emissions compared to the MEIC. The power plants in the MEIC present the very low emissions of BC and OC, particularly for OC with 0.0 kt, resulting largely from the high uncertainties in the emission factor of these species (Zhao et al., 2011, 2015; Zhou et al., 2017). Furthermore, the MEIC power plant emissions of SO₂, PM_{2.5}, PM₁₀, and NO_x shared with the larger fractions of 28.8, 11.3, 11.6 and 35.4 %, respectively to CO, BC, OC, and NMVOCs with the fractions of 3.7, 0.2, 0.0, and 0.4 %, in the total emissions (Table 1). When the UEIPP was introduced to MEIC by replacing the original power plant emission, the UEIPP contributed 10.4, 3.7, 4.0, 17.2, 6.2, 4.3, 1.7, and 0.9 %, to the total emissions of SO₂, PM_{2.5}, PM₁₀, NO_x, CO, BC, OC, and NMVOCs, respectively. The ratios of PM_{2.5} (3.7 %) and PM₁₀ (4.0 %) of the UEIPP were comparable to the ratios of 4 % for PM_{2.5} and 6 % for PM₁₀ calculated by Zhou et al. (2017).

The spatial difference of the two emission inventories over Jiangsu Province is shown in Fig. 2, as well as their absolute values in Fig. S1 in the Supplement. The UEIPP presented low emissions of SO₂, PM_{2.5}, PM₁₀, and NO_x in most areas (Fig. 2a–d), and the high emissions of CO, BC, OC, and NMVOCs in urban areas over the province (Fig. 2e–h). The two inventories exhibited similar spatial distribution patterns with large emissions in southern and low emissions in middle and northern Jiangsu (Fig. S1 in the Supplement). The power plants around Xuzhou, an industrial city, formed a high emission center over northwestern Jiangsu (Fig. S1 in the Supplement).

To assess the simulation performance with the UEIPP and changes in the atmospheric environment over Jiangsu Province under the updated emission conditions, simulations with the original MEIC emission inventory (hereinafter referred to as the MOD1 simulation) and the updated MEIC emission inventory with the power generation replaced by UEIPP (hereinafter referred to as the MOD2 simulation) were carried out. The difference in chemical components be-

tween MOD1 and MOD2 simulations were used to assess atmospheric environmental changes in the following sections.

3 Modeling evaluation

3.1 Meteorological evaluation

An evaluation of the meteorological simulations over the domain with 5 km horizontal resolution was carried out in regards to temperature, relative humidity (RH), and wind speed and direction in Nanjing, Yancheng, and Lianyungang. The evaluation of statistical parameters included mean bias (MB), correlation coefficient (R), and root mean square error (RMSE; Table 2). The R and RMSE of temperature in the three cities ranged from 0.86 to 0.94 (p values < 0.001) and 2.0 to 3.0 °C, respectively, showing a close agreement between the simulation and observations. MB values of temperature manifested a slight underestimate in Nanjing (-1.0 °C) and Lianyungang (-0.5 °C), and an overestimate in Yancheng (1.1 °C). The R of RH were 0.79, 0.79, and 0.82 (p values < 0.001), with the RMSE values of 14.6, 14.4, and 18.2 % in Nanjing, Yancheng, and Lianyungang, respectively, which were comparable to previous studies (Gao et al., 2016a; Liu et al., 2016). The MB of RH was positive in Nanjing and Lianyungang, but negative in Yancheng. The variations in wind speed were generally captured by the model with the R varying from 0.51 to 0.77 (p values < 0.001). The RMSE of wind speed ranged from 1.8 to 2.1 m s⁻¹, basically conforming to the “good” model performance criteria for wind speed (less than 2.0 m s⁻¹; Emery et al., 2001). Wind directions were evaluated via hit rates (HR; Schlünzen and Sokhi, 2008) with desired accuracy between $\pm 45^\circ$. The HR values were 63, 64, and 49 % in Nanjing, Yancheng, and Lianyungang, respectively, indicating that variations in wind direction were basically captured. Generally, the meteorological fields in Jiangsu Province were reasonably reproduced by WRF-Chem during the simulation period.

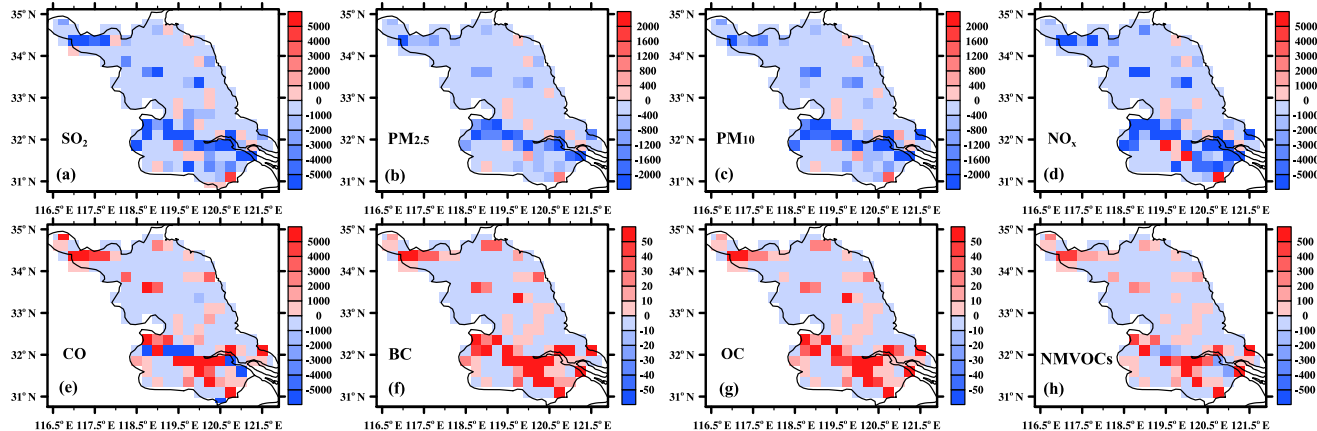
3.2 Chemical evaluation

The surface observations of PM_{2.5}, CO, NO₂, O₃, and SO₂ at 13 urban sites in Jiangsu (Fig. 1b) were collected for evaluating the chemical simulation over the domain with 5 km horizontal resolution in MOD1 and MOD2. Three statistical parameters of R, mean fractional bias (MFB) and mean frac-

Table 3. Statistics comparing observed and simulated PM_{2.5}, CO, NO₂, O₃, and SO₂.

| | R | | MFB (%) | | MFE (%) | |
|-------------------|-------|-----------|---------|-------------|---------|------------|
| | MOD1 | MOD2 | MOD1 | MOD2 | MOD1 | MOD2 |
| PM _{2.5} | 0.568 | 0.571↑ | -8.31 | -8.24↑ | 45.40 | 45.65 |
| CO | 0.516 | 0.515 | -36.05 | -35.84↑ | 52.05 | 52.10 |
| NO ₂ | 0.456 | 0.466↑ | 14.08 | 10.48↑** | 39.37 | 38.77↑ |
| O ₃ | 0.600 | 0.625↑*** | -121.46 | -110.68↑*** | 131.74 | 124.67↑*** |
| SO ₂ | 0.260 | 0.261↑ | 24.88 | 16.62↑*** | 65.18 | 63.20↑* |

* all R values passed $p < 0.001$; Up arrows indicate the chemical simulation results in MOD2 are improved;
***, **, and * indicate the improvements are statistically significant with confidence levels of 99, 95, and 90 %, respectively. Equations of R, MFB, and MFE were provided in the Supplement.

**Figure 2.** Differences in power plant emissions between MEIC and UEIPP in 2012 (units: tons).**Table 4.** Validation statistics of SIAs in PM_{2.5} at Nanjing.

| | NMB (%) | | NME (%) | |
|----------|---------|---------|---------|--------|
| | MOD1 | MOD2 | MOD1 | MOD2 |
| Sulfate | -87.61 | -87.29↑ | 87.61 | 87.29↑ |
| Nitrate | -19.47 | -16.38↑ | 29.06 | 28.61↑ |
| Ammonium | -55.12 | -53.47↑ | 55.12 | 53.47↑ |

* Up arrows indicate the same meaning as in Table 3. Equations of NMB and NME were provided in the Supplement.

tional error (MFE) were presented in Table 3. The MFB and MFE could normalize bias and error for simulated–observed pairs ranging from -200 to 200 % and from 0 to 200 %, respectively, indicating their appropriateness to evaluate performance over a wide range of concentrations (Boylan and Russell, 2006). Normalized mean bias (NMB) and normalized mean error (NME) by individual site and air pollutant were additionally presented in Table S1 in the Supplement. As shown in Table 3, the values of MFB and MFE indicate that the hourly variations in PM_{2.5}, CO, and NO₂ were reasonably captured by both MOD1 and MOD2 simulations, conforming to the “satisfactory” criteria proposed by Mor-

ris et al. (2005) that MFB is within ± 60 % and MFE is below 75 %. Given a high dependence on emissions, the deviations of CO and NO₂ concentrations could be largely resulting from their emission uncertainties. The high R and the negative MFB of O₃ indicate the hourly variations were reasonably captured but undervalued systematically, especially at night (Fig. 9b; Fig. S2 in the Supplement). The CBM-Z scheme and the outdated land-use data from the United States Geological Survey (USGS) were prone to undervalue the surface O₃ concentrations in association with producing high NO titration and dry deposition, respectively (Balzarini et al., 2015; Park et al., 2014). Similar underestimations were previously simulated in eastern China (Gao et al., 2015; Liao et al., 2015; L. Wang et al., 2016). The mean NMB and NME of O₃ in MOD1, calculated at -53.97 and 67.00 %, respectively (Table S1 in the Supplement), were comparable to previous China studies (Li et al., 2012; Tang et al., 2015; L. Wang et al., 2016; Zhou et al., 2017), while the mean NMB and NME of O₃ in MOD2 were ameliorated to -45.83 and 63.61 %, respectively. The SO₂ changes were generally captured in the two simulations in terms of MFB and MFE, but with an overestimation and a low R. In addition to emissions, the absence of pathways converting SO₂ to sulfate in the current WRF-Chem model, such as aqueous-phase oxidation of dis-

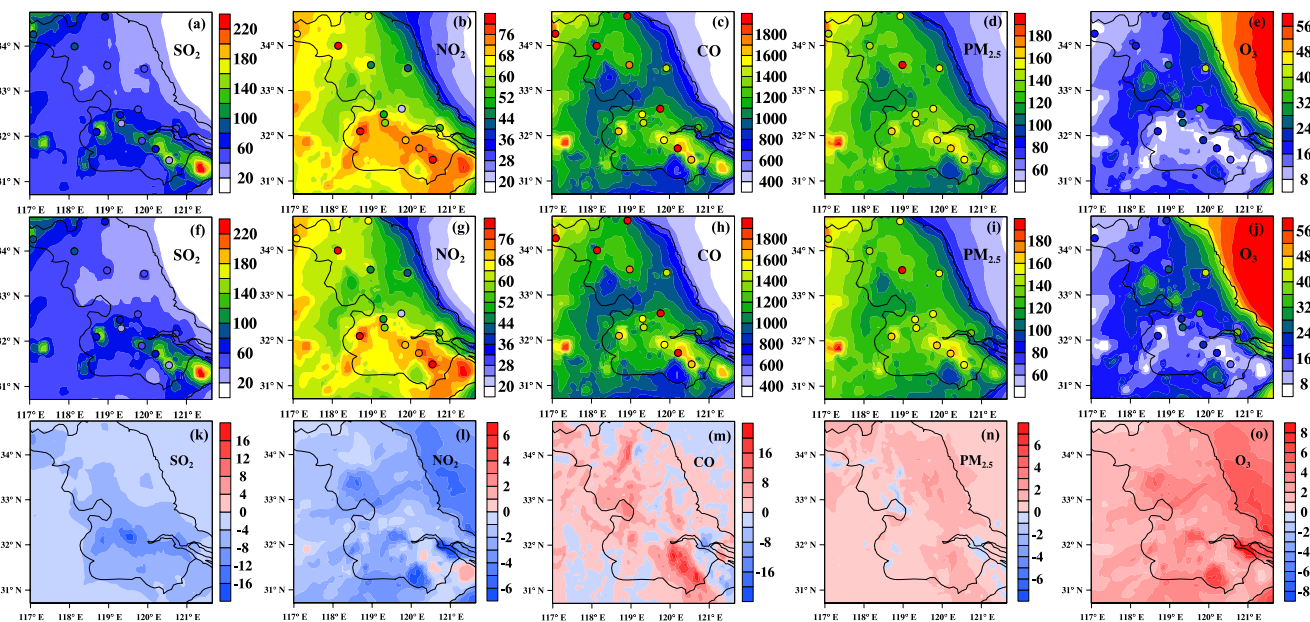


Figure 3. The spatial distributions of near-surface SO_2 , NO_2 , CO , $\text{PM}_{2.5}$, and O_3 concentrations ($\mu\text{g m}^{-3}$) from (a–e) MOD1, (f–j) MOD2 and (k–o) the differences between MOD2 and MOD1 averaged over December 2013. The observed concentrations were indicated by colored circles.

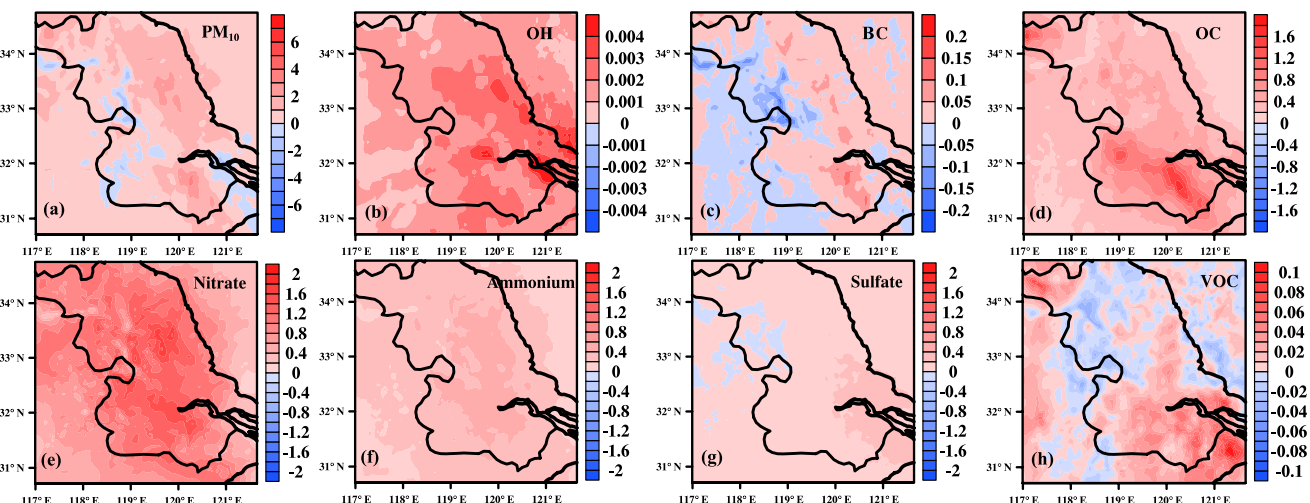


Figure 4. Differences in chemical species between MOD2 and MOD1 in December 2013. Unit: “pptv” for OH ; “ppmv” for VOC ; “ $\mu\text{g m}^{-3}$ ” for the others.

solved $\text{S}_{(\text{IV})}$ (the sum of hydrated $\text{SO}_2 - \text{SO}_2 \cdot \text{H}_2\text{O}$, bisulfite – HSO_3^- , and sulfite – SO_3^{2-}) by dissolved NO_2 under conditions of high ammonia (NH_3) and NO_2 concentrations (X. Huang et al., 2014; Xue et al., 2016; He et al., 2014), was partially responsible for the simulation deviations of SO_2 and NO_2 . Aerosols in east Asia are featured with low acidity due to the high NH_3 and mineral dust emissions capturing more acidic gases (SO_2 and NO_x) under moist air conditions during haze episodes (Cheng et al., 2016; G. Wang et

al., 2016). The modeled SIAs at the Nanjing site (Fig. 1b) were assessed in addition. As can be seen from Table 4 and Fig. S3a in the Supplement, the simulated sulfate concentrations were obviously underestimated, providing further evidence for the above-mentioned speculation. Similar underestimation of sulfate was also found in the North China Plain (Gao et al., 2016a, b). The observed nitrate and ammonium concentrations were comparatively well caught, particularly the NMBs of nitrate ranged within $\pm 20\%$ in the two simula-

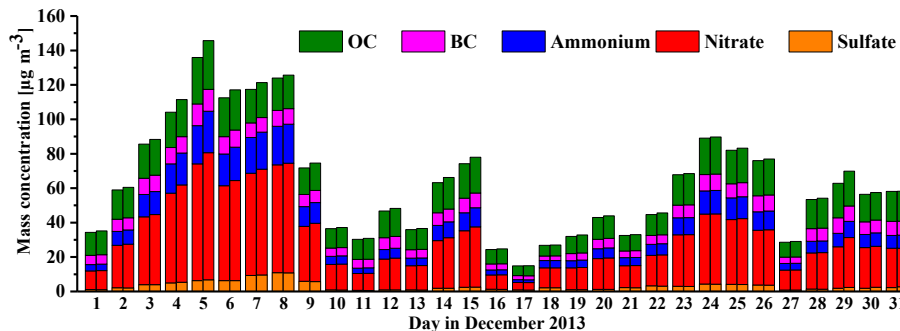


Figure 5. Chemical species of $\text{PM}_{2.5}$ simulated in MOD1 (left bar of each bar pair) and MOD2 (right bar of each bar pair) in December 2013.

tions. In general, the chemical observations were reasonably captured by both simulations of MOD1 and MOD2.

The R , MFB, and MFE in the MOD1 and MOD2 simulations were presented in Table 3 with an overall assessment of simulation with the UEIPP. A better simulation performance is reflected by higher R , smaller absolute value of MFB, and lower MFE, respectively tagged with upward arrows in Table 3. Additionally, significance of the improvements between the statistical indices was checked by using the method of bootstrap confidence interval (DiCiccio and Efron, 1996; He et al., 2017). In response to the introduction of UEIPP, chemical simulation showed a comprehensive improvement in MOD2 (see the upward arrows in Table 3). Although both MOD1 and MOD2 underestimated $\text{PM}_{2.5}$, CO , O_3 , and overestimated NO_2 and SO_2 as shown in Table 3, the MFBs for those species reduced by 0.07, 0.21, 10.78, 3.6, and 8.26 % from MOD1 to MOD2. The improvements of O_3 , SO_2 , and NO_2 were statistically significant (Table 3). For the O_3 simulation, the improvements of the R , MFB, and MFE significantly passed the confidence level of 99 %. For the SO_2 simulation, the improvements of MFB and MFE passed the confidence levels of 99 and 90 %, respectively. Improvement in MFB of NO_2 was significant at the 95 % confidence level. Also, the modeled SIAs were ameliorated in the MOD2 simulation (Table 4). Under the unchanged meteorology between the two simulations, the reduced deviations of NO_2 , SO_2 , CO , $\text{PM}_{2.5}$, and O_3 in MOD2 relative to MOD1 could be attributed to the emission changes with UEIPP. However, $\text{PM}_{2.5}$ and O_3 are highly dependent on secondary formation, indicating the changes in chemical conversion in the simulations of MOD1 and MOD2, which was more comprehensively investigated in Sect. 4.

Spatially, overestimates of SO_2 in MOD1 mainly occurred in southern urban areas and Xuzhou (Fig. 3a), where the SO_2 overestimates were mostly improved in MOD2 (Fig. 3k, f). For the NO_2 simulation, the overestimates lay in the majority of cities throughout Jiangsu Province with a few cities underestimated such as Suzhou (Fig. 3b), and were mitigated correspondingly in MOD2 as well (Fig. 3l, g). As a common feature of the MOD1 simulation, CO , $\text{PM}_{2.5}$, and O_3 were un-

dervalued throughout most city sites (Fig. 3c–e), while in response to the usage of UEIPP, their concentrations in MOD2 were comprehensively improved (Fig. 3h–j, m–o).

As mentioned above, MOD2 with the introduction of UEIPP improved the simulation of air pollutants, especially of O_3 , SO_2 , and NO_2 according to model performance evaluation. It is therefore concluded that the power plant emissions of UEIPP are more realistic.

4 Environmental changes under the updated emission conditions

4.1 Influence of emission changes on air pollutant modeling

Aside from introducing the updated emission inventories, another important and meaningful work in this study is to explore how the emission changes affect the atmospheric environment, especially in severe haze episodes, for understanding the complexity of the atmospheric environment. To this end, we presented the differences in atmospheric compositions simulated with MOD1 and MOD2 in Fig. 4. Consistently with the emission changes (Fig. 2), the concentrations were reduced for SO_2 and NO_2 (Fig. 3k, l), and enhanced for BC and OC (Fig. 4c, d) in most areas. However, it is not yet clear what was responsible for the enhanced O_3 concentration in MOD2, and why the $\text{PM}_{2.5}$ concentration enhanced when the $\text{PM}_{2.5}$ primary emission largely reduced, which are urgently needed to address especially for the abnormal increase in $\text{PM}_{2.5}$, since more implemented restrictions on power plants are being executed in East China.

As a secondary air pollutant in the boundary layer, O_3 is highly subjected to its precursors (Ou Yang et al., 2012; Gao et al., 2005). The Yangtze River Delta was characterized as VOC-limited, especially in winter, indicating O_3 concentrations were depressed by NO_x and sensitive to VOCs (Liu et al., 2010; Wang et al., 2008; Tie et al., 2013). The ratio of $\text{HCHO} / \text{NO}_y$, an indicator to differentiate VOC-limited ($\text{HCHO} / \text{NO}_y < 0.28$) and NO_x -limited ($\text{HCHO} / \text{NO}_y > 0.28$) conditions, verified Jiangsu Province

Table 5. Increased concentrations ($\mu\text{g m}^{-3}$) of $\text{PM}_{2.5}$, total of BC and OC, and total of SOA (sulfate, nitrate, and ammonium) from MOD1 to MOD2 averaged over Jiangsu Province with the percentage differences between MOD1 and MOD2 compared with MOD1.

| | $\text{PM}_{2.5}$ | $\text{BC} + \text{OC}$ | Sulfate + nitrate + ammonium |
|----------------------|-------------------|-------------------------|------------------------------|
| Hazy days (3–8 Dec) | 3.38 (1.81 %) | 1.04 (3.06 %) | 4.77 (5.11 %) |
| The whole (1–31 Dec) | 1.03 (0.83 %) | 0.58 (2.38 %) | 1.32 (3.96 %) |

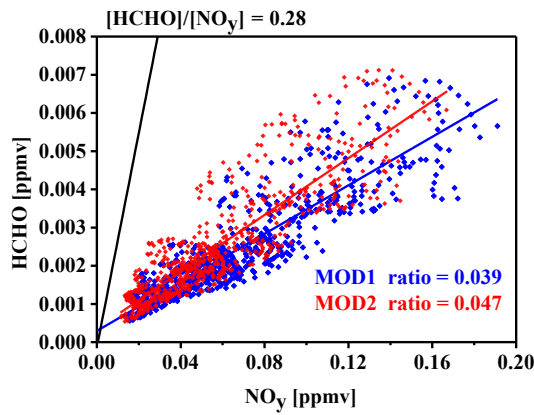


Figure 6. Ratios of $\text{HCHO} / \text{NO}_y$ simulated in MOD1 (blue) and MOD2 (red).

as a VOC-limited region during the modeling period (Fig. 6). Therefore, either the increase in VOCs or the decrease in NO_x could enhance the surface O_3 level. Coincidentally, the concentrations of VOCs and NO_2 increased and decreased, respectively, (Figs. 3l and 4h), following their emission changes in UEIPP (Table 1). In addition, a high anti-correlation relationship existed between the spatial changes in O_3 and NO_2 (Fig. 3l, o) as well as the diurnal changes (Fig. 9a, b). Therefore, we could partially attribute the underestimated O_3 to the emission uncertainties of VOC and NO_2 in the original MEIC. Furthermore, as a precursor of O_3 , high CO concentrations in MOD2, with the updated MEIC emission inventory, would contribute to the enhancement of O_3 concentration as well.

Quite surprising to us, the surface $\text{PM}_{2.5}$ concentrations did not follow the reducing emissions of primary $\text{PM}_{2.5}$, but increased over almost all the province (Fig. 3n). As $\text{PM}_{2.5}$ is highly dependent on three factors: primary emissions, physical processes, and chemical reactions in the atmosphere, the latter two factors were more likely to dominate in the simulation of increased $\text{PM}_{2.5}$ concentrations. Due to the strong absorbing effects of BC on solar radiation and the higher rejection height of power plants, the enhancement of BC concentrations (Fig. 4c) would reduce solar radiation to the ground, and thus suppressing vertical diffusion and accumulating more pollutants near the surface. The speculation could be verified by reductions of downward short-wave

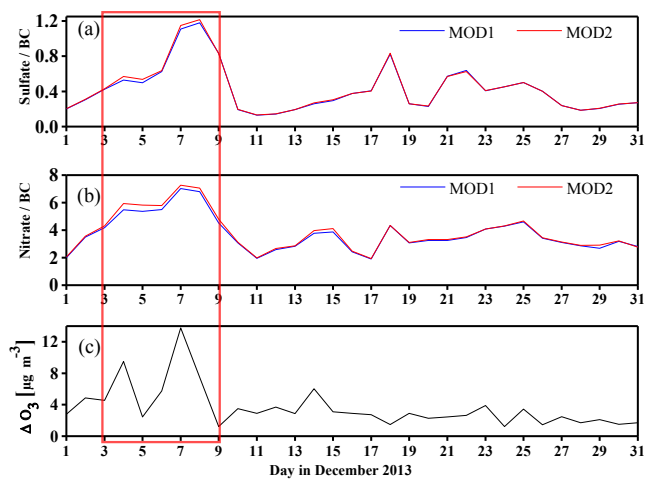


Figure 7. Daily variations in (a) sulfate / BC, (b) nitrate / BC, and (c) difference in O_3 (MOD2–MOD1) averaged over Jiangsu with the red rectangular column marking the severe haze episode (3–8 December); the increase of sulfate / BC and nitrate/BC suggests enhanced chemical productions.

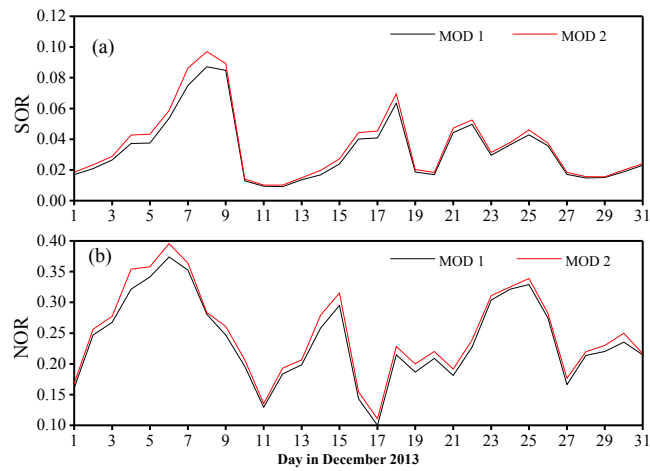


Figure 8. Daily variations in (a) molar ratio of sulfate to sum of sulfate and SO_2 (SOR) and (b) molar ratio of nitrate to sum of nitrate and NO_2 (NOR).

flux at the ground surface (SWDOWN), 2 m air temperature, and boundary layer height. Regionally averaged over Jiangsu

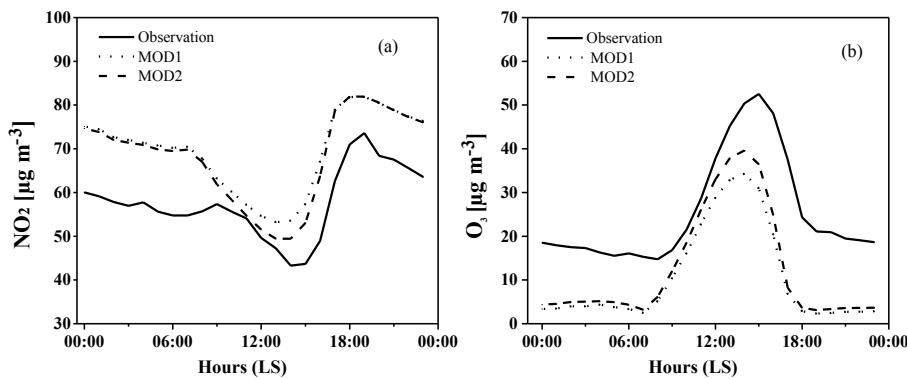


Figure 9. Diurnal variations in (a) NO_2 and (b) O_3 averaged over 13 cities in Jiangsu Province (Fig. 1b).

Province during 1–31 December, the SWDOWN, 2 m temperature and boundary layer height reduced by 0.65 W m^{-2} , 0.005°C , and 0.4 m , respectively, and the reductions became more significant to 11.8 W m^{-2} , 0.3°C , and 26.4 m , respectively, during the daytime of 7 December 2013 in Wuxi, a haze center, increasing air stability for more air pollutant accumulation. In order to quantify the radiative effects induced by BC emission change, a sensitivity test MODa (same as MOD2) with closing BC emission in UEIPP was performed. Based on the $\text{PM}_{2.5}$ differences between MOD2 and MODa regionally averaged over Jiangsu Province, it was estimated that the BC aerosol radiative effect stabilizing boundary layer contributed only about $0.15 \mu\text{g m}^{-3}$ to the $\text{PM}_{2.5}$ enhancements, during the haze episode.

4.2 Reinforcing atmospheric oxidation capacity and enhancing SIAs

As described in Sect. 4.1, the declined emissions of primary $\text{PM}_{2.5}$ could not improve the ambient $\text{PM}_{2.5}$ concentration and the feedback aerosol radiative effects on aerosol change were weak, implying the contribution of chemical production to the $\text{PM}_{2.5}$ enhancement. In this section, the chemical production of SIAs was analyzed since the CBM-Z and MOSAIC coupled model used in WRF-Chem is incapable of simulating SOA formation. Previous studies had revealed that SIAs played an important role in $\text{PM}_{2.5}$, particularly in the haze pollution over eastern China (R.-J. Huang et al., 2014; Wang et al., 2014; Gao et al., 2016b). Given the reduction of SO_2 and NO_x emissions in the UEIPP, the simulated sulfate and nitrate should be lower from the oxidation of SO_2 and NO_2 . However, as shown in Fig. 4, both sulfate and nitrate are increased in MOD2, and more significantly during the haze episode (3–8 December; Fig. 5). In the atmosphere, sulfate is formed through oxidation of SO_2 by gas-phase reactions with OH (Stockwell and Calvert, 1983; Blitz et al., 2003) and stabilized Criegee intermediate formed by O_3 and alkenes (Mauldin III et al., 2012) as well as by heterogeneous reactions with H_2O_2 , O_3 , OH, organic peroxides, and various oxides of nitrogen in clouds (Seinfeld and Pandis, 2012). Ni-

trate is mostly formed from the gas-phase reactions of NO_2 with OH during daylight and heterogeneous reactions of nitrate radical (NO_3) at night. Therefore, the formations of secondary sulfate and nitrate depend not only on their precursors but also on the oxidizing capacity of the atmosphere.

As major oxidizing agents in the atmosphere, O_3 and OH were increased from MOD1 to MOD2 (Figs. 3a and 4b), indicating the enhanced oxidizing capacity in MOD2 relative to MOD1 in the Jiangsu region. A WRF-Chem/RADM2 simulation was performed as well because changes in OH and VOC oxidation in the presence of NO_x are sensitive to chemistry mechanisms (Derwent, 2017; Knote et al., 2015; Stockwell et al., 2011; Jimenez et al., 2003). The similar pattern of increasing O_3 and OH were found over the province (Fig. S4 in the Supplement), which could further indicate the enhanced oxidizing capacity.

To evaluate how the formation of secondary aerosols responded to the enhanced oxidizing capacity, we analyzed the BC-scaled concentrations for sulfate and nitrate. The purpose was to eliminate the influence of air pollutant dilution and mixing in the atmospheric physical process. Since BC is quite inert to chemical reactions, its variations could well reflect the atmospheric physical processes. Thus, the BC-scaled concentration could better represent the contribution of chemical reactions (Zheng et al., 2015). Figure 7 presents the daily averaged variation in BC-scaled concentrations for sulfate and nitrate, appending the differences in O_3 as an indicator for the change of atmospheric oxidizing capacity. As revealed in Fig. 7, the enhancements of chemical production simulated in MOD2 were well consistent with the variations of O_3 difference between MOD2 and MOD1. During the haze episode of 3–8 December 2013, the chemical production of sulfate and nitrate enhanced obviously, which is in accordance with the rapid build-up of O_3 , indicating the chemical production is intensified by strengthening of oxidizing capacity during the episode. It is worth pointing out that photochemical activity is generally reduced by weakening solar radiation from high aerosol levels during the severe haze period in China. Our modeling study also confirmed the rela-

tively low ozone concentrations during the haze period from 3–8 December 2013 in Jiangsu Province, and furthermore found the UEIPP led to enhanced atmospheric oxidizing capacity during the haze periods in East China, which could result from changing photochemical oxidation of VOC, NO_x, and SO₂ from regional industrial sources (Guo et al., 2014). Large particle-mass growth was observed concurrently with elevated daily ozone concentrations throughout the PM_{2.5} episodes in China, indicating the importance of photochemical activity in the secondary aerosol production (Guo et al., 2014).

The SOR (molar ratio of sulfate to sum of sulfate and SO₂) and NOR (molar ratio of nitrate to sum of nitrate and NO₂) were used as indicators of secondary transformation (Sun et al., 2006), since the BC-scaled concentrations just represent the intensity of chemical reaction effects, overlooking the precursors for individual compounds. The SOR and NOR would give insights into the chemical transformation of SO₂ and NO_x. As shown in Fig. 8, the chemical transformations from SO₂ and NO_x to sulfate and nitrate were always strengthened during the whole month in MOD2, that could be why the chemical production of sulfate and nitrate in MOD2 increased (Fig. 7a, b) even with less precursor concentrations. Additionally, in response to the enhanced atmospheric oxidizing agents, the secondary ammonium was also increased (Fig. 4f) under the same NH₃ emission conditions in MOD1 and MOD2.

As shown in Table 5, the total concentration of sulfate, nitrate and ammonium increased by 1.32 µg m⁻³ during the whole month of 1–31 December 2013 and even reached up to 4.77 µg m⁻³ in the haze episode of 3–8 December 2013, higher than the increments of PM_{2.5} as well as the total increments of BC and OC, which could clearly reveal that the enhancement of SIAs in response to the reinforced atmospheric oxidizing capacity contributed the majority to the increased PM_{2.5} concentrations. This conclusion was verified by an emission sensitivity study in the North China Plain performed by L. Wang et al. (2016), who found that the 30 % emission reduction of NO_x led to a notable increase in PM_{2.5} concentrations contributing to NH₃-rich and VOC-limited conditions in the winter.

It should interpret the larger enhancement in concentrations of SIAs than the PM_{2.5} in Table 5. Compared to the MOD1, the lower emission of primary PM_{2.5} in UEIPP (Table 1) leads to less concentrations of primary PM_{2.5} in MOD2, and the enhancement in concentrations of SIAs was partially offset by the lower primary concentrations of PM_{2.5}.

5 Conclusions

Power plants, as major air pollutant sources in China, have been imposed with restrictions by the government in response to the increasing air pollution, which led power plant emissions to large variations during the past few years. Due

to various underlying data and approaches, there remained uncertainties in estimating the power plant emissions. In the present study, the UEIPP in Jiangsu Province for 2012 was introduced into the MEIC emission inventory as the major point sources. The variation and complexity of the atmospheric environment in response to the change of power plant emissions over Jiangsu were studied by executing the WRF-Chem simulations using the original emissions of MEIC and the MEIC with its power plant emission inventory updated by the UEIPP.

This study focused on the uncertainties in estimating the power plant emissions. In the UEIPP, the emission amounts of SO₂, PM_{2.5}, PM₁₀, NO_x, CO, BC, OC, and NMVOCs were 105.6, 21.6, 32.6, 277.9, 582.0, 3.6, 2.5, and 17.3 kt, respectively, manifesting obvious differences with the MEIC emission inventory. Uncertainties in meteorology (MET) and chemistry (CHEM), two other major uncertainties in numerical simulations of fine urban PM, were excluded with optimally selected meteorological and chemical settings based on the meteorological and chemical validations of the MOD1 simulation comparing to the observations. There are challenges for the development of atmospheric chemical models with the MET, especially in planetary boundary layer parameterizations, such as the key role of aging of BC in the interaction between pollution and the planetary boundary layer (Peng et al., 2016), and CHEM including enhanced aqueous chemistry during the development of severe haze in China (R. Zhang et al., 2015). Further modeling work could consider these MET and CHEM issues based on the new understandings of atmospheric physical and chemical processes.

The UEIPP drove the simulation performance to be superior to the original power plant emission of the MEIC inventory in terms of the proximity between simulated and observed air pollutant concentrations, suggesting a more realistic power plant emission inventory. The complexity of the atmospheric environment was also revealed by comparing the changes in various primary and secondary compositions in the atmosphere. Atmospheric oxidizing capacity was reinforced in response to the enhancement of O₃ and OH, which was largely due to higher VOC emissions and lower NO_x in the UEIPP. PM_{2.5} increased almost all over Jiangsu Province, even the primary emission reduced by 7.6 %. This phenomenon was mainly attributed to the enhanced formation of SIAs, induced by the enhanced atmospheric oxidizing capacity, revealing the complex mechanism of air pollution from fine particulate matter to atmospheric oxidants. Reduction of SO₂ may free NH₃ to react instead with NO_x creating ammonium nitrate particles, which would need further studying. Our study also quantified the PM_{2.5} enhancement in response to the BC radiative effect stabilizing the boundary layer. The chemical reaction was more dominant in PM_{2.5} enhancement than the BC radiative effect.

Given the complicated processes in environmental change, the restrictions of emissions should be comprehensively considered rather than one single factor. Furthermore, the effects

of emission inventories on air-quality variations could be assessed based on long-term observation and simulation studies, and formation of SOAs would also enhance due to the reinforced atmospheric oxidizing capacity and higher VOC emissions.

Data availability. Data used in this manuscript can be provided upon request by email to Lei Zhang (leiz002@126.com) or Tianliang Zhao (josef_zhao@126.com).

The Supplement related to this article is available online at <https://doi.org/10.5194/acp-18-2065-2018-supplement>.

Competing interests. The authors declare that they have no conflict of interest.

Acknowledgements. This study was jointly funded by National Key R & D Program Pilot Projects of China (2016YFC0203304); Key program for Environmental Protection of Jiangsu Province in 2015 (2015017); Program of Multi-Scale Haze-fog Modeling Development of National Science & Technology Support Program (2014BAC16B03); and the Program for Postgraduates Research and Innovation in Universities of Jiangsu Province (KYLX16_0937).

Edited by: Renyi Zhang

Reviewed by: two anonymous referees

References

- Amnuaylojaroen, T., Barth, M. C., Emmons, L. K., Carmichael, G. R., Kreasuwun, J., Prasitwattanaseree, S., and Chantara, S.: Effect of different emission inventories on modeled ozone and carbon monoxide in Southeast Asia, *Atmos. Chem. Phys.*, 14, 12983–13012, <https://doi.org/10.5194/acp-14-12983-2014>, 2014.
- Balzarini, A., Pirovano, G., Honzak, L., Žabkar, R., Curci, G., Forkel, R., Hirtl, M., San José, R., Tuccella, P., and Grell, G.: WRF-Chem model sensitivity to chemical mechanisms choice in reconstructing aerosol optical properties, *Atmos. Environ.*, 115, 604–619, 2015.
- Blitz, M. A., Hughes, K. J., and Pilling, M. J.: Determination of the high-pressure limiting rate coefficient and the enthalpy of reaction for OH + SO₂, *J. Phys. Chem. A*, 107, 1971–1978, 2003.
- Bo, Y., Cai, H., and Xie, S.: Spatial and temporal variation of historical anthropogenic NMVOCs emission inventories in China, *Atmos. Chem. Phys.*, 8, 7297–7316, <https://doi.org/10.5194/acp-8-7297-2008>, 2008.
- Boylan, J. W. and Russell, A. G.: PM and light extinction model performance metrics, goals, and criteria for three-dimensional air quality models, *Atmos. Environ.*, 40, 4946–4959, <https://doi.org/10.1016/j.atmosenv.2005.09.087>, 2006.
- Carter, W. P. L.: Development of an improved chemical speciation database for processing emissions of volatile organic compounds for air quality models, report available at: <http://www.engr.ucr.edu/~carter/emitdb/> (last access: April 2016), 2013.
- Cheng, Y., Zheng, G., Wei, C., Mu, Q., Zheng, B., Wang, Z., Gao, M., Zhang, Q., He, K., and Carmichael, G.: Reactive nitrogen chemistry in aerosol water as a source of sulfate during haze events in China, *Sci. Adv.*, 2, e1601530, <https://doi.org/10.1126/sciadv.1601530>, 2016.
- Derwent, R.: Intercomparison of chemical mechanisms for air quality policy formulation and assessment under North American conditions, *J. Air Waste Manage. Assoc.*, 67, 1–8, 2017.
- DiCiccio, T. J. and Efron, B.: Bootstrap confidence intervals, *Stat. Sci.*, 11, 189–212, 1996.
- Emery, C., Tai, E., and Yarwood, G.: Enhanced meteorological modeling and performance evaluation for two Texas ozone episodes, prepared for the Texas Near Non-Attainment Areas through the Alamo Area Council of Governments, by ENVIRON International Corp, Novato, CA, http://www.tnrc.state.tx.us/air/aqp/airquality_contracts.html#met01 (last access: January 2017), 2001.
- Fu, Q., Zhuang, G., Wang, J., Xu, C., Huang, K., Li, J., Hou, B., Lu, T., and Streets, D. G.: Mechanism of formation of the heaviest pollution episode ever recorded in the Yangtze River Delta, China, *Atmos. Environ.*, 42, 2023–2036, <https://doi.org/10.1016/j.atmosenv.2007.12.002>, 2008.
- Fu, X., Wang, S., Zhao, B., Xing, J., Cheng, Z., Liu, H., and Hao, J.: Emission inventory of primary pollutants and chemical speciation in 2010 for the Yangtze River Delta region, China, *Atmos. Environ.*, 70, 39–50, <https://doi.org/10.1016/j.atmosenv.2012.12.034>, 2013.
- Gao, J., Wang, T., Ding, A., and Liu, C.: Observational study of ozone and carbon monoxide at the summit of mount Tai (1534 m a.s.l.) in central-eastern China, *Atmos. Environ.*, 39, 4779–4791, <https://doi.org/10.1016/j.atmosenv.2005.04.030>, 2005.
- Gao, J., Zhu, B., Xiao, H., Kang, H., Hou, X., and Shao, P.: A case study of surface ozone source apportionment during a high concentration episode, under frequent shifting wind conditions over the Yangtze River Delta, China, *Sci. Total Environ.*, 544, 853–863, <https://doi.org/10.1016/j.scitotenv.2015.12.039>, 2015.
- Gao, M., Carmichael, G. R., Wang, Y., Saide, P. E., Yu, M., Xin, J., Liu, Z., and Wang, Z.: Modeling study of the 2010 regional haze event in the North China Plain, *Atmos. Chem. Phys.*, 16, 1673–1691, <https://doi.org/10.5194/acp-16-1673-2016>, 2016a.
- Gao, M., Carmichael, G. R., Wang, Y., Ji, D., Liu, Z., and Wang, Z.: Improving simulations of sulfate aerosols during winter haze over Northern China: the impacts of heterogeneous oxidation by NO₂, *Front. Environ. Sci. Eng.*, 10, 16, <https://doi.org/10.1007/s11783-016-0878-2>, 2016b.
- Guenther, A., Karl, T., Harley, P., Wiedinmyer, C., Palmer, P. I., and Geron, C.: Estimates of global terrestrial isoprene emissions using MEGAN (Model of Emissions of Gases and Aerosols from Nature), *Atmos. Chem. Phys.*, 6, 3181–3210, <https://doi.org/10.5194/acp-6-3181-2006>, 2006.
- Guo, S., Hu, M., Zamora, M. L., Peng, J., Shang, D., Zheng, J., Du, Z., Wu, Z., Shao, M., Zeng, L., Mario J. M., and Zhang, R.: Elucidating severe urban haze formation in China, *P. Natl. Acad. Sci. USA*, 111, 17373–17378, 2014.

- Hao, J., Tian, H., and Lu, Y.: Emission inventories of NO_x from commercial energy consumption in China, 1995–1998, *Environ. Sci. Technol.*, 36, 552–560, 2002.
- He, H., Wang, Y., Ma, Q., Ma, J., Chu, B., Ji, D., Tang, G., Liu, C., Zhang, H., and Hao, J.: Mineral dust and NO_x promote the conversion of SO_2 to sulfate in heavy pollution days, *Sci. Rep.*, 4, 4172, <https://doi.org/10.1038/srep04172>, 2014.
- He, J., Wu, L., Mao, H., Liu, H., Jing, B., Yu, Y., Ren, P., Feng, C., and Liu, X.: Development of a vehicle emission inventory with high temporal–spatial resolution based on NRT traffic data and its impact on air pollution in Beijing – Part 2: Impact of vehicle emission on urban air quality, *Atmos. Chem. Phys.*, 16, 3171–3184, <https://doi.org/10.5194/acp-16-3171-2016>, 2016.
- He, J. J., Yu, Y., Yu, L. J., Liu, N., and Zhao, S. P.: Impacts of uncertainty in land surface information on simulated surface temperature and precipitation over China, *Int. J. Climatol.*, 37, 829–847, <https://doi.org/10.1002/joc.5041>, 2017.
- Hong, S.-Y., Noh, Y., and Dudhia, J.: A new vertical diffusion package with an explicit treatment of entrainment processes, *Mon. Weather Rev.*, 134, 2318–2341, 2006.
- Hu, X.-M., Klein, P. M., Xue, M., Zhang, F., Doughty, D. C., Forkel, R., Joseph, E., and Fuentes, J. D.: Impact of the vertical mixing induced by low-level jets on boundary layer ozone concentration, *Atmos. Environ.*, 70, 123–130, <https://doi.org/10.1016/j.atmosenv.2012.12.046>, 2013.
- Huang, C., Chen, C. H., Li, L., Cheng, Z., Wang, H. L., Huang, H. Y., Streets, D. G., Wang, Y. J., Zhang, G. F., and Chen, Y. R.: Emission inventory of anthropogenic air pollutants and VOC species in the Yangtze River Delta region, China, *Atmos. Chem. Phys.*, 11, 4105–4120, <https://doi.org/10.5194/acp-11-4105-2011>, 2011.
- Huang, R.-J., Zhang, Y., Bozzetti, C., Ho, K.-F., Cao, J.-J., Han, Y., Daellenbach, K. R., Slowik, J. G., Platt, S. M., and Canonaco, F.: High secondary aerosol contribution to particulate pollution during haze events in China, *Nature*, 514, 218–222, 2014.
- Huang, X., Song, Y., Zhao, C., Li, M., Zhu, T., Zhang, Q., and Zhang, X.: Pathways of sulfate enhancement by natural and anthropogenic mineral aerosols in China, *J. Geophys. Res.-Atmos.*, 119, 14165–14179, <https://doi.org/10.1002/2014JD022301>, 2014.
- Iacono, M. J., Delamere, J. S., Mlawer, E. J., Shephard, M. W., Clough, S. A., and Collins, W. D.: Radiative forcing by long-lived greenhouse gases: Calculations with the AER radiative transfer models, *J. Geophys. Res.-Atmos.*, 113, D13103, <https://doi.org/10.1029/2008jd009944>, 2008.
- Janssens-Maenhout, G., Crippa, M., Guizzardi, D., Dentener, F., Muntean, M., Pouliot, G., Keating, T., Zhang, Q., Kurokawa, J., and Wankmüller, R.: HTAP_v2. 2: a mosaic of regional and global emission grid maps for 2008 and 2010 to study hemispheric transport of air pollution, *Atmos. Chem. Phys.*, 15, 11411–11432, <https://doi.org/10.5194/acp-15-11411-2015>, 2015.
- Jiangsu Bureau of Statistics (JSNBS): Statistical Yearbook of Jiangsu, Beijing, China Statistics Press, 2013.
- Jimenez, P., Baldasano, J. M., and Dabdub, D.: Comparison of photochemical mechanisms for air quality modeling, *Atmos. Environ.*, 37, 4179–4194, 2003.
- Jing, B., Wu, L., Mao, H., Gong, S., He, J., Zou, C., Song, G., Li, X., and Wu, Z.: Development of a vehicle emission inventory with high temporal–spatial resolution based on NRT traffic data and its impact on air pollution in Beijing – Part 1: Development and evaluation of vehicle emission inventory, *Atmos. Chem. Phys.*, 16, 3161–3170, <https://doi.org/10.5194/acp-16-3161-2016>, 2016.
- Kalnay, E., Kanamitsu, M., Kistler, R., Collins, W., Deaven, D., Gandin, L., Iredell, M., Saha, S., White, G., and Woollen, J.: The NCEP/NCAR 40-year reanalysis project, *B. Am. Meteorol. Soc.*, 77, 437–471, 1996.
- Knote, C., Tuccella, P., Curci, G., Emmons, L., Orlando, J. J., Madronich, S., Baró, R., Jiménez-Guerrero, P., Luecken, D., and Hogrefe, C.: Influence of the choice of gas-phase mechanism on predictions of key gaseous pollutants during the AQMEII phase-2 intercomparison, *Atmos. Environ.*, 115, 553–568, 2015.
- Li, L., Chen, C., Huang, C., Huang, H., Zhang, G., Wang, Y., Wang, H., Lou, S., Qiao, L., and Zhou, M.: Process analysis of regional ozone formation over the Yangtze River Delta, China using the Community Multi-scale Air Quality modeling system, *Atmos. Chem. Phys.*, 12, 10971–10987, <https://doi.org/10.5194/acp-12-10971-2012>, 2012.
- Li, M., Zhang, Q., Streets, D. G., He, K. B., Cheng, Y. F., Emmons, L. K., Huo, H., Kang, S. C., Lu, Z., Shao, M., Su, H., Yu, X., and Zhang, Y.: Mapping Asian anthropogenic emissions of non-methane volatile organic compounds to multiple chemical mechanisms, *Atmos. Chem. Phys.*, 14, 5617–5638, <https://doi.org/10.5194/acp-14-5617-2014>, 2014.
- Liao, J., Wang, T., Jiang, Z., Zhuang, B., Xie, M., Yin, C., Wang, X., Zhu, J., Fu, Y., and Zhang, Y.: WRF/Chem modeling of the impacts of urban expansion on regional climate and air pollutants in Yangtze River Delta, China, *Atmos. Environ.*, 106, 204–214, <https://doi.org/10.1016/j.atmosenv.2015.01.059>, 2015.
- Liu, F., Zhang, Q., Tong, D., Zheng, B., Li, M., Huo, H., and He, K. B.: High-resolution inventory of technologies, activities, and emissions of coal-fired power plants in China from 1990 to 2010, *Atmos. Chem. Phys.*, 15, 13299–13317, <https://doi.org/10.5194/acp-15-13299-2015>, 2015.
- Liu, J., Mauzerall, D. L., Chen, Q., Zhang, Q., Song, Y., Peng, W., Klimont, Z., Qiu, X., Zhang, S., Hu, M., Lin, W., Smith, K. R., and Zhu, T.: Air pollutant emissions from Chinese households: A major and underappreciated ambient pollution source, *P. Natl. Acad. Sci. USA*, 113, 7756–7761, <https://doi.org/10.1073/pnas.1604537113>, 2016.
- Liu, S., McKeen, S., Hsie, E. Y., Lin, X., Kelly, K., Bradshaw, J., Sandholm, S., Browell, E., Gregory, G., and Sachse, G.: Model study of tropospheric trace species distributions during PEM-West A, *J. Geophys. Res.-Atmos.*, 101, 2073–2085, 1996.
- Liu, X.-H., Zhang, Y., Xing, J., Zhang, Q., Wang, K., Streets, D. G., Jang, C., Wang, W.-X., and Hao, J.-M.: Understanding of regional air pollution over China using CMAQ, part II. Process analysis and sensitivity of ozone and particulate matter to precursor emissions, *Atmos. Environ.*, 44, 3719–3727, <https://doi.org/10.1016/j.atmosenv.2010.03.036>, 2010.
- Mauldin III, R., Berndt, T., Sipilä, M., Paasonen, P., Petäjä, T., Kim, S., Kurten, T., Stratmann, F., Kerminen, V.-M., and Kulmala, M.: A new atmospherically relevant oxidant of sulphur dioxide, *Nature*, 488, 193–196, 2012.
- Morris, R. E., McNally, D. E., Tesche, T. W., Tonnesen, G., Boylan, J. W., and Brewer, P.: Preliminary Evaluation of the Community Multiscale Air Quality Model for 2002 over the Southeast-

- ern United States, J. Air Waste Manage. Assoc., 55, 1694–1708, <https://doi.org/10.1080/10473289.2005.10464765>, 2005.
- Morrison, H., Thompson, G., and Tatarskii, V.: Impact of cloud microphysics on the development of trailing stratiform precipitation in a simulated squall line: Comparison of one-and two-moment schemes, Mon. Weather Rev., 137, 991–1007, 2009.
- National Bureau of Statistics (NBS): China Statistical Yearbook 2013, China Statistics Press, Beijing, 2013.
- Ohara, T., Akimoto, H., Kurokawa, J.-I., Horii, N., Yamaji, K., Yan, X., and Hayasaka, T.: An Asian emission inventory of anthropogenic emission sources for the period 1980–2020, Atmos. Chem. Phys., 7, 4419–4444, <https://doi.org/10.5194/acp-7-4419-2007>, 2007.
- Olivier, J. G., Van Aardenne, J. A., Dentener, F. J., Pagliari, V., Ganzeveld, L. N., and Peters, J. A.: Recent trends in global greenhouse gas emissions: regional trends 1970–2000 and spatial distribution of key sources in 2000, Environ. Sci., 2, 81–99, 2005.
- Ou Yang, C.-F., Lin, N.-H., Sheu, G.-R., Lee, C.-T., and Wang, J.-L.: Seasonal and diurnal variations of ozone at a high-altitude mountain baseline station in East Asia, Atmos. Environ., 46, 279–288, <https://doi.org/10.1016/j.atmosenv.2011.09.060>, 2012.
- Park, R. J., Hong, S. K., Kwon, H. A., Kim, S., Guenther, A., Woo, J. H., and Loughner, C. P.: An evaluation of ozone dry deposition simulations in East Asia, Atmos. Chem. Phys., 14, 7929–7940, <https://doi.org/10.5194/acp-14-7929-2014>, 2014.
- Peng, J., Hu, M., Guo, S., Du, Z., Zheng, J., Shang, D., Zamora, M. L., Zeng, L., Shao, M., and Wu, Y.-S.: Markedly enhanced absorption and direct radiative forcing of black carbon under polluted urban environments, P. Natl. Acad. Sci. USA, 113, 4266–4271, 2016.
- Qi, X. M., Ding, A. J., Nie, W., Petäjä, T., Kerminen, V. M., Herrmann, E., Xie, Y. N., Zheng, L. F., Manninen, H., Aalto, P., Sun, J. N., Xu, Z. N., Chi, X. G., Huang, X., Boy, M., Virkkula, A., Yang, X. Q., Fu, C. B., and Kulmala, M.: Aerosol size distribution and new particle formation in the western Yangtze River Delta of China: 2 years of measurements at the SORPES station, Atmos. Chem. Phys., 15, 12445–12464, <https://doi.org/10.5194/acp-15-12445-2015>, 2015.
- Schultz, M.: REanalysis of the TROpospheric chemical composition over the past 40 years (RETRO), A long-term global modeling study of tropospheric chemistry funded under the 5th EU Framework Programme, Final Report, Jülich/Hamburg, available at http://retro-archive.iek.fz-juelich.de/data/documents/reports/D5-3_final.pdf (last access: November 2016), 2007.
- Schlünzen, K. H. and Sokhi, R. S.: Overview of tools and methods for meteorological and air pollution mesoscale model evaluation and user training, Joint report by WMO and COST 728, WMO/TD-No. 1457, Geneva, Switzerland, Electronic version: November 2008, 2008.
- Seinfeld, J. H. and Pandis, S. N.: Atmospheric chemistry and physics: from air pollution to climate change, Chapter 01: The atmosphere, John Wiley & Sons, 2012.
- Stauffer, D. R. and Seaman, N. L.: Use of four-dimensional data assimilation in a limited-area mesoscale model. Part I: Experiments with synoptic-scale data, Mon. Weather Rev., 118, 1250–1277, [https://doi.org/10.1175/1520-0493\(1990\)118<1250:uofdda>2.0.co;2](https://doi.org/10.1175/1520-0493(1990)118<1250:uofdda>2.0.co;2), 1990.
- Stockwell, W. R. and Calvert, J. G.: The mechanism of the HO-SO₂ reaction, Atmos. Environ., 17, 2231–2235, 1983.
- Stockwell W. R., Middleton, P., Chang, J. S., and Tang, X.: The second generation Regional Acid Deposition Model chemical mechanism for regional air quality modeling, J. Geophys. Res., 95, 16343–16367, 1990.
- Stockwell, W. R., Lawson, C. V., Saunders, E., and Goliff, W. S.: A review of tropospheric atmospheric chemistry and gas-phase chemical mechanisms for air quality modeling, Atmosphere, 3, 1–32, 2011.
- Streets, D. G., Zhang, Q., Wang, L., He, K., Hao, J., Wu, Y., Tang, Y., and Carmichael, G. R.: Revisiting China's CO emissions after the transport and chemical evolution over the Pacific (TRACE-P) mission: synthesis of inventories, atmospheric modeling, and observations, J. Geophys. Res.-Atmos., 111, 1–16, <https://doi.org/10.1029/2006jd007118>, 2006.
- Sun, Y., Zhuang, G., Tang, A., Wang, Y., and An, Z.: Chemical characteristics of PM_{2.5} and PM₁₀ in haze-fog episodes in Beijing, Environ. Sci. Technol., 40, 3148–3155, 2006.
- Tang, Y., An, J., Wang, F., Li, Y., Qu, Y., Chen, Y., and Lin, J.: Impacts of an unknown daytime HONO source on the mixing ratio and budget of HONO, and hydroxyl, hydroperoxyl, and organic peroxy radicals, in the coastal regions of China, Atmos. Chem. Phys., 15, 9381–9398, <https://doi.org/10.5194/acp-15-9381-2015>, 2015.
- Tian, H., Liu, K., Hao, J., Wang, Y., Gao, J., Qiu, P., and Zhu, C.: Nitrogen oxides emissions from thermal power plants in China: Current status and future predictions, Environ. Sci. Technol., 47, 11350–11357, 2013.
- Tie, X., Geng, F., Guenther, A., Cao, J., Greenberg, J., Zhang, R., Apel, E., Li, G., Weinheimer, A., Chen, J., and Cai, C.: Megacity impacts on regional ozone formation: observations and WRF-Chem modeling for the MIRAGE-Shanghai field campaign, Atmos. Chem. Phys., 13, 5655–5669, <https://doi.org/10.5194/acp-13-5655-2013>, 2013.
- Wang, G., Zhang, R., Gomez, M. E., Yang, L., Levy Zamora, M., Hu, M., Lin, Y., Peng, J., Guo, S., Meng, J., Li, J., Cheng, C., Hu, T., Ren, Y., Wang, Y., Gao, J., Cao, J., An, Z., Zhou, W., Li, G., Wang, J., Tian, P., Marrero-Ortiz, W., Secret, J., Du, Z., Zheng, J., Shang, D., Zeng, L., Shao, M., Wang, W., Huang, Y., Wang, Y., Zhu, Y., Li, Y., Hu, J., Pan, B., Cai, L., Cheng, Y., Ji, Y., Zhang, F., Rosenfeld, D., Liss, P. S., Duce, R. A., Kolb, C. E., and Molina, M. J.: Persistent sulfate formation from London Fog to Chinese haze, P. Natl. Acad. Sci. USA, <https://doi.org/10.1073/pnas.1616540113>, 2016.
- Wang, H., An, J., Shen, L., Zhu, B., Pan, C., Liu, Z., Liu, X., Duan, Q., Liu, X., and Wang, Y.: Mechanism for the formation and microphysical characteristics of submicron aerosol during heavy haze pollution episode in the Yangtze River Delta, China, Sci. Total Environ., 490, 501–508, <https://doi.org/10.1016/j.scitotenv.2014.05.009>, 2014.
- Wang, L., Zhang, Y., Wang, K., Zheng, B., Zhang, Q., and Wei, W.: Application of Weather Research and Forecasting Model with Chemistry (WRF/Chem) over northern China: Sensitivity study, comparative evaluation, and policy implications, Atmos. Environ., 124, 337–350, <https://doi.org/10.1016/j.atmosenv.2014.12.052>, 2016.
- Wang, L. T., Zhang, Q., Hao, J. M., and He, K. B.: Anthropogenic CO emission inventory of Mainland China, Acta Sci. Cir., 25, 1580–1585, 2005.

- Wang, M., Cao, C., Li, G., and Singh, R. P.: Analysis of a severe prolonged regional haze episode in the Yangtze River Delta, China, *Atmos. Environ.*, 102, 112–121, 2015.
- Wang, Q., Han, Z., Wang, T., and Zhang, R.: Impacts of biogenic emissions of VOC and NO_x on tropospheric ozone during summertime in eastern China, *Sci. Total Environ.*, 395, 41–49, <https://doi.org/10.1016/j.scitotenv.2008.01.059>, 2008.
- Wang, S., Zhao, M., Xing, J., Wu, Y., Zhou, Y., Lei, Y., He, K., Fu, L., and Hao, J.: Quantifying the air pollutants emission reduction during the 2008 Olympic Games in Beijing, *Environ. Sci. Technol.*, 44, 2490–2496, 2010.
- Wang, S. W., Zhang, Q., Streets, D. G., He, K. B., Martin, R. V., Lamsal, L. N., Chen, D., Lei, Y., and Lu, Z.: Growth in NO_x emissions from power plants in China: bottom-up estimates and satellite observations, *Atmos. Chem. Phys.*, 12, 4429–4447, <https://doi.org/10.5194/acp-12-4429-2012>, 2012.
- Xia, Y., Zhao, Y., and Nielsen, C. P.: Benefits of China's efforts in gaseous pollutant control indicated by the bottom-up emissions and satellite observations 2000–2014, *Atmos. Environ.*, 136, 43–53, 2016.
- Xue, J., Yuan, Z., Griffith, S. M., Yu, X., Lau, A. K. H., and Yu, J. Z.: Sulfate Formation Enhanced by a Cocktail of High NO_x, SO₂, Particulate Matter, and Droplet pH during Haze-Fog Events in Megacities in China: An Observation-Based Modeling Investigation, *Environ. Sci. Technol.*, 50, 7325–7334, <https://doi.org/10.1021/acs.est.6b00768>, 2016.
- Zaveri, R. A.: A new lumped structure photochemical mechanism for large-scale applications, *J. Geophys. Res.*, 104, 30387–30415, 1999.
- Zaveri, R. A., Easter, R. C., Fast, J. D., and Peters, L. K.: Model for Simulating Aerosol Interactions and Chemistry (MOSAIC), *J. Geophys. Res.*, 113, D13204, <https://doi.org/10.1029/2007jd008782>, 2008.
- Zhang, Q., Streets, D. G., He, K., and Klimont, Z.: Major components of China's anthropogenic primary particulate emissions, *Environ. Res. Lett.*, 2, 045027, <https://doi.org/10.1088/1748-9326/2/4/045027>, 2007a.
- Zhang, Q., Streets, D. G., He, K., Wang, Y., Richter, A., Burrows, J. P., Uno, I., Jang, C. J., Chen, D., and Yao, Z.: NO_x emission trends for China, 1995–2004: The view from the ground and the view from space, *J. Geophys. Res.-Atmos.*, 112, D22306, <https://doi.org/10.1029/2007JD008684>, 2007b.
- Zhang, Q., Streets, D. G., Carmichael, G. R., He, K., Huo, H., Kanani, A., Klimont, Z., Park, I., Reddy, S., and Fu, J.: Asian emissions in 2006 for the NASA INTEX-B mission, *Atmos. Chem. Phys.*, 9, 5131–5153, <https://doi.org/10.5194/acp-9-5131-2009>, 2009.
- Zhang, Q., Yan, R., Fan, J., Yu, S., Yang, W., and Li, P., Wang, S., Chen, B., Liu, W., and Zhang, X.: A Heavy Haze Episode in Shanghai in December of 2013: Characteristics, Origins and Implications, *Aerosol Air Qual. Res.*, 15, 1881–1893, <https://doi.org/10.4209/aaqr.2015.03.0179>, 2015.
- Zhang, R., Wang, G., Guo, S., Zamora, M. L., Ying, Q., Lin, Y., Wang, W., Hu, M., and Wang, Y.: Formation of urban fine particulate matter, *Chem. Rev.*, 115, 3803–3855, 2015.
- Zhang, Y., Kong, S., Tang, L., Zhao, T., Han, Y., and Yu, H.: Analysis on Emission Inventory and Temporal-Spatial Characteristics of Pollutants from Key Coal-Fired Stationary Sources in Jiangsu Province by On-Line Monitoring Data, *Environ. Sci.*, 36, 2775–2783, 2015.
- Zhao, Y., Wang, S., Duan, L., Lei, Y., Cao, P., and Hao, J.: Primary air pollutant emissions of coal-fired power plants in China: Current status and future prediction, *Atmos. Environ.*, 42, 8442–8452, <https://doi.org/10.1016/j.atmosenv.2008.08.021>, 2008.
- Zhao, Y., Wang, S., Nielsen, C. P., Li, X., and Hao, J.: Establishment of a database of emission factors for atmospheric pollutants from Chinese coal-fired power plants, *Atmos. Environ.*, 44, 1515–1523, <https://doi.org/10.1016/j.atmosenv.2010.01.017>, 2010.
- Zhao, Y., Nielsen, C. P., Lei, Y., McElroy, M. B., and Hao, J.: Quantifying the uncertainties of a bottom-up emission inventory of anthropogenic atmospheric pollutants in China, *Atmos. Chem. Phys.*, 11, 2295–2308, <https://doi.org/10.5194/acp-11-2295-2011>, 2011.
- Zhao, Y., Qiu, L. P., Xu, R. Y., Xie, F. J., Zhang, Q., Yu, Y. Y., Nielsen, C. P., Qin, H. X., Wang, H. K., Wu, X. C., Li, W. Q., and Zhang, J.: Advantages of a city-scale emission inventory for urban air quality research and policy: the case of Nanjing, a typical industrial city in the Yangtze River Delta, China, *Atmos. Chem. Phys.*, 15, 12623–12644, <https://doi.org/10.5194/acp-15-12623-2015>, 2015.
- Zheng, G. J., Duan, F. K., Su, H., Ma, Y. L., Cheng, Y., Zheng, B., Zhang, Q., Huang, T., Kimoto, T., Chang, D., Pöschl, U., Cheng, Y. F., and He, K. B.: Exploring the severe winter haze in Beijing: the impact of synoptic weather, regional transport and heterogeneous reactions, *Atmos. Chem. Phys.*, 15, 2969–2983, <https://doi.org/10.5194/acp-15-2969-2015>, 2015.
- Zheng, J., Zhang, L., Che, W., Zheng, Z., and Yin, S.: A highly resolved temporal and spatial air pollutant emission inventory for the Pearl River Delta region, China and its uncertainty assessment, *Atmos. Environ.*, 43, 5112–5122, <https://doi.org/10.1016/j.atmosenv.2009.04.060>, 2009.
- Zhou, Y., Zhao, Y., Mao, P., Zhang, Q., Zhang, J., Qiu, L., and Yang, Y.: Development of a high-resolution emission inventory and its evaluation and application through air quality modeling for Jiangsu Province, China, *Atmos. Chem. Phys.*, 17, 211–233, <https://doi.org/10.5194/acp-17-211-2017>, 2017.